

Trap-center recombination processes by rare earth activators in YAlO₃ single crystal hostA. Vedda,¹ M. Fasoli,¹ M. Nikl,² V. V. Laguta,² E. Mihokova,^{1,2} J. Pejchal,² A. Yoshikawa,³ and M. Zhuravleva³¹*Dipartimento di Scienza dei Materiali, Università di Milano–Bicocca, Via Cozzi 53, 20125 Milano, Italy*²*Institute of Physics, ASCR, Cukrovarnicka 10, 162 53 Prague, Czech Republic*³*IMRAM, Tohoku University, 2-1-1 Katahira, Aoba-ku, 980-8577 Sendai, Japan*

(Received 22 December 2008; revised manuscript received 11 May 2009; published 16 July 2009)

The trapping-recombination processes occurring in YAlO₃ single crystals are investigated by wavelength-resolved thermally stimulated luminescence (TSL) studies from 10 to 300 K after x-ray irradiation at 10 K. Undoped crystals and crystals doped with rare earth ions are studied. The results obtained on undoped, Yb³⁺-, Eu³⁺-, and Tm³⁺-doped samples indicate the existence of seven glow peaks due to intrinsic hole traps. Three of them (at 154, 190, and 232 K) are related to different variants of O⁻ centers, as demonstrated by the correspondence between the thermal stabilities of such centers detected by electron paramagnetic resonance and the glow peak temperatures. From the analysis of the TSL emission spectra it is found that rare earth ions, after capturing electrons during irradiation, play the role of recombination centers. The thermal depths and the room-temperature lifetimes of the traps are also evaluated. After doping with rare earth ions which are expected to act as hole traps such as Ce³⁺, Pr³⁺, and Tb³⁺ only one main peak is observed, preceded by a nearly temperature-independent emission which is completely suppressed at temperatures higher than the glow peak temperature. For each particular dopant the peak coincides with one of those observed in the undoped crystal while the TSL spectral emission is characteristic of the rare earth ion dopant. To interpret such results we suggest the existence of defect complexes, involving intrinsic defects coupled to Ce³⁺, Pr³⁺, and Tb³⁺ rare earth ions, in which carriers can be transferred from intrinsic levels to the rare earth ion levels, where the radiative recombination occurs.

DOI: [10.1103/PhysRevB.80.045113](https://doi.org/10.1103/PhysRevB.80.045113)

PACS number(s): 78.60.Kn, 61.72.-y, 78.20.-e, 42.70.-a

I. INTRODUCTION

Scintillators are materials able to efficiently convert ionizing radiations into UV-visible photons, thus allowing their measurement by light detectors. Applications of scintillators are extensively found in medical imaging, industrial and security controls, and high-energy physics experiments.

It is usually considered that the overall efficiency η of a scintillator can be expressed by the formula $\eta = \beta S Q$,¹ where β is the efficiency of conversion of an incident photon or particle into e - h pairs, S is the efficiency of carrier transfer toward the luminescent center, and Q is the luminescence efficiency of the center. While β and Q are determined, respectively, by the choice of the material and of the activator (or of the intrinsic transition if an intrinsic scintillator is considered), the term S strongly depends upon lattice defects and it can considerably vary in crystals with the same nominal composition but with different quality. Therefore, the investigation and control of defects acting as traps of free carriers is recognized as an important stage in scintillator research.

According to the thermal depth of traps with respect to the conduction or valence bands, the mean time spent by carriers in traps at room temperature (RT) can vary in an extremely wide time scale, from μ s-ms or even less up to years. The effect of traps on scintillation varies accordingly: shallow traps with decay times on the order of μ s to ms induce slow tails in the scintillation decay of fast scintillators, like those exploiting the $5d$ - $4f$ transition of Ce³⁺ whose decay time lies in the ns time scale. Otherwise, deep traps keep the carriers for such long times that they cannot be monitored in scintillation measurements while they reduce the overall efficiency of a scintillator. One should note that the terms “shallow”

and “deep” are not uniquely defined. The same trap in a material can be considered shallow or deep depending on the time scale of optical transitions.

The case of Y-Al perovskite (YAlO₃, commonly denoted as YAP) is particularly interesting for what concerns the investigation of traps. Besides laser applications, Ce-doped YAP crystals are thoroughly studied for their use as scintillators both in bulk form grown by the Czochralski method²⁻⁴ and, recently, as thin films prepared by liquid phase epitaxy.⁵ Moreover, also Pr³⁺ (Refs. 6 and 7) and Yb³⁺ (Refs. 8-11) dopings were explored. The heavier LuAlO₃:Ce analog (LuAP:Ce) was grown as well,¹² however, since its growth is rather difficult, alternatively mixed Y_{1-x}Lu_xAP:Ce crystals with x up to 0.8 were considered and successfully obtained.¹³⁻¹⁶

The role of defects in the scintillation properties of YAP and LuAP was soon recognized and several papers appeared, some of them directly relating traps monitored by thermally stimulated luminescence (TSL) to the temperature dependence of the scintillation signal. It turned out that traps detected by TSL at cryogenic temperatures have a direct role in shaping the temperature dependence of the scintillation intensity. The higher light yield of YAP:Ce with respect to LuAP:Ce, as well as the presence of a scintillation rise time in LuAP:Ce were explained in terms of a different distribution of shallow traps in the two materials.¹⁷⁻²⁰ Deeper traps monitored by TSL above RT were found to reduce the overall transfer efficiency in these scintillator materials, even if additional nonradiative recombination processes are presumably also present.²¹

Since traps are detrimental for scintillator applications, material engineering should focus on their elimination; the question of their nature is a crucial point in order to guide

material preparation and to avoid simple trial and error experiments. The study of the defect character in perovskites was approached by both experimental and theoretical tools, where theoretical efforts were also aimed at a direct comparison with existing experimental results. By atomistic simulations it was found that among point defects, cation antisites (aluminum ions at yttrium site or vice versa) are characterized by the lowest formation energy and they are the dominant intrinsic defects in YAP and LuAP, followed by cation and anion vacancies (Schottky disorder).^{22,23} Cationic nonstoichiometry should lead preferentially to antisite disorder too.²³ Since Y (or Lu) and Al are isovalent, in principle, antisite defects are not expected to act as traps for charged carriers; however, recent density-functional calculations showed that Al ions at Y (or Lu) sites give rise to electron traps about 0.4–0.8 eV below the conduction-band edge.²⁴ Moreover, the positive role of Zr codoping in reducing the TSL of YAP:Ce crystals²⁵ was explained by the incorporation of this codopant as ZrO₂ consequently compensating oxygen vacancies acting as traps in the lattice.²⁶

Experimental efforts aimed at understanding the nature of defects involved especially electron-paramagnetic-resonance (EPR) and TSL studies. Following a previous EPR work, where O⁻ defects (holes trapped at oxygen sites) were found in YAP at cryogenic temperatures after visible or UV irradiation,²⁷ their structure was further investigated and up to five variants with different thermal stabilities were detected. Three of them were correlated with TSL peaks observed below RT. Oxygen-vacancy-based traps were detected as well and it was preliminary suggested that TSL recombination could occur between holes thermally freed from O⁻ defects and electrons trapped at oxygen vacancy sites. Moreover, extrinsic defects such as Ti³⁺ and Mo³⁺ were also observed.²⁸ While below RT oxygen vacancies with trapped electrons are stable and probably play the role of recombination centers in the TSL process, their thermal stability is reduced above RT; the glow peaks monitored by TSL above RT were ascribed to the recombination of electrons detrapped from oxygen vacancies with holes trapped at Ce⁴⁺ centers via a thermally stimulated tunneling mechanism.²⁹

So far, studies specifically devoted to TSL were carried on samples doped with Ce³⁺ due to the scintillator application of YAP:Ce crystals. TSL data of crystals doped with other activators such as Yb³⁺ and Pr³⁺ were also reported:^{6,7,9,10} the shape of the TSL glow curves appeared to be influenced by doping but the data were considered mainly from the application point of view. A detailed investigation of the TSL patterns when different rare earth ions are involved is missing. To tackle the topic, in this paper we compare the TSL properties of both undoped and doped YAP crystals at low temperatures. A rich variety of dopants (such as Eu, Tm, Yb, Ce, Pr, and Tb) was considered in order to provide a more complete picture of the nature of the recombination processes occurring in YAP crystals. Moreover, we evaluate the depth of traps associated with the observed TSL peaks and discuss their influence in the scintillation decay processes.

II. EXPERIMENTAL CONDITIONS

The crystals considered in this study are (i) one undoped and one Ce-doped crystal (0.5 at %) grown by Czochralski

technique with 4N purity starting materials from molybdenum crucible in CRYTUR Ltd. (Czech Republic); (ii) several rare earth doped crystals grown in IMRAM, Tohoku University (Japan) by the micropulling down method with 4N purity starting materials from iridium crucible and with rare earth concentrations of 0.01 at % and 0.1 at % for Ce³⁺, 0.1 at % for Eu³⁺, Tm³⁺, and Pr³⁺, and 2 at % for Yb³⁺. All the concentrations refer to the melt. Small differences are expected to occur between concentrations in the melt and in the crystal due to the close-to-one high segregation coefficients of the rare earth ions considered in YAP host. Moreover, a few measurements were also performed on one undoped sample grown by Czochralski technique by CRYTUR and on one undoped sample grown by the micropulling down method by IMRAM with 5N and 4N purity starting materials, respectively. For the measurements, plates were cut with dimensions 7×3×1 mm³ and polished up to an optical grade.

TSL measurements in the 10–310 K range were performed after x-ray irradiation at 10 K by a Philips 2274 x-ray tube operated at 20 kV. The x-ray doses imparted for the measurements were on the order of 10¹ Gy; moreover we verified that a linear dependence of the TSL signal amplitudes occurs from approximately 1 up to 200 Gy. The TSL apparatus consisted in a homemade spectrometer measuring the TSL intensity as a function of both the temperature and wavelength. The detection system was a monochromator (TRIAx 180 Jobin-Yvon) coupled to a charge-coupled-device detector (Jobin-Yvon Spectrum One 3000) operating in the 190–1100 nm interval. The spectral resolution was about 5 nm. The TSL emission spectra were corrected for the spectral efficiency of the detection system. A 0.1 K/s heating rate was adopted.

III. EXPERIMENTAL RESULTS AND DISCUSSION

A. Undoped crystals and crystals doped with Yb³⁺, Eu³⁺, and Tm³⁺

In this section we present TSL results relative to samples doped with those rare earth ions which, due to their electronic configuration, preferentially trap electrons during irradiation so as to modify their charge state from 3+ to 2+; moreover the results on such crystals are compared to those obtained for undoped samples. Wavelength-resolved TSL measurements are displayed in Figs. 1(a)–1(d), where the contour plots obtained after irradiation at 10 K are reported for the Czochralski grown undoped (4N purity starting materials), 2% Yb³⁺-doped, 0.1% Eu³⁺-doped, and 0.1% Tm³⁺-doped crystals, respectively. The contour plot of only one undoped sample is reported as an example, due to the strong similarity among the three investigated crystals. A rich variety of TSL peaks is observed in all samples, extending from 10–20 K up to RT. The peak temperatures are similar in different samples while the nature of the emission centers changes according to doping. A selection of TSL emission spectra obtained by integration of wavelength-resolved measurements in specific temperature intervals is reported in Fig. 2. We observe (i) the $4f^{12} {}^3P_0 - 4f^{12} {}^3H_J$ and the $4f^{12} {}^1D_2 - 4f^{12} {}^3H_6$ emission lines of Tm³⁺ in the Tm³⁺-doped crystal;

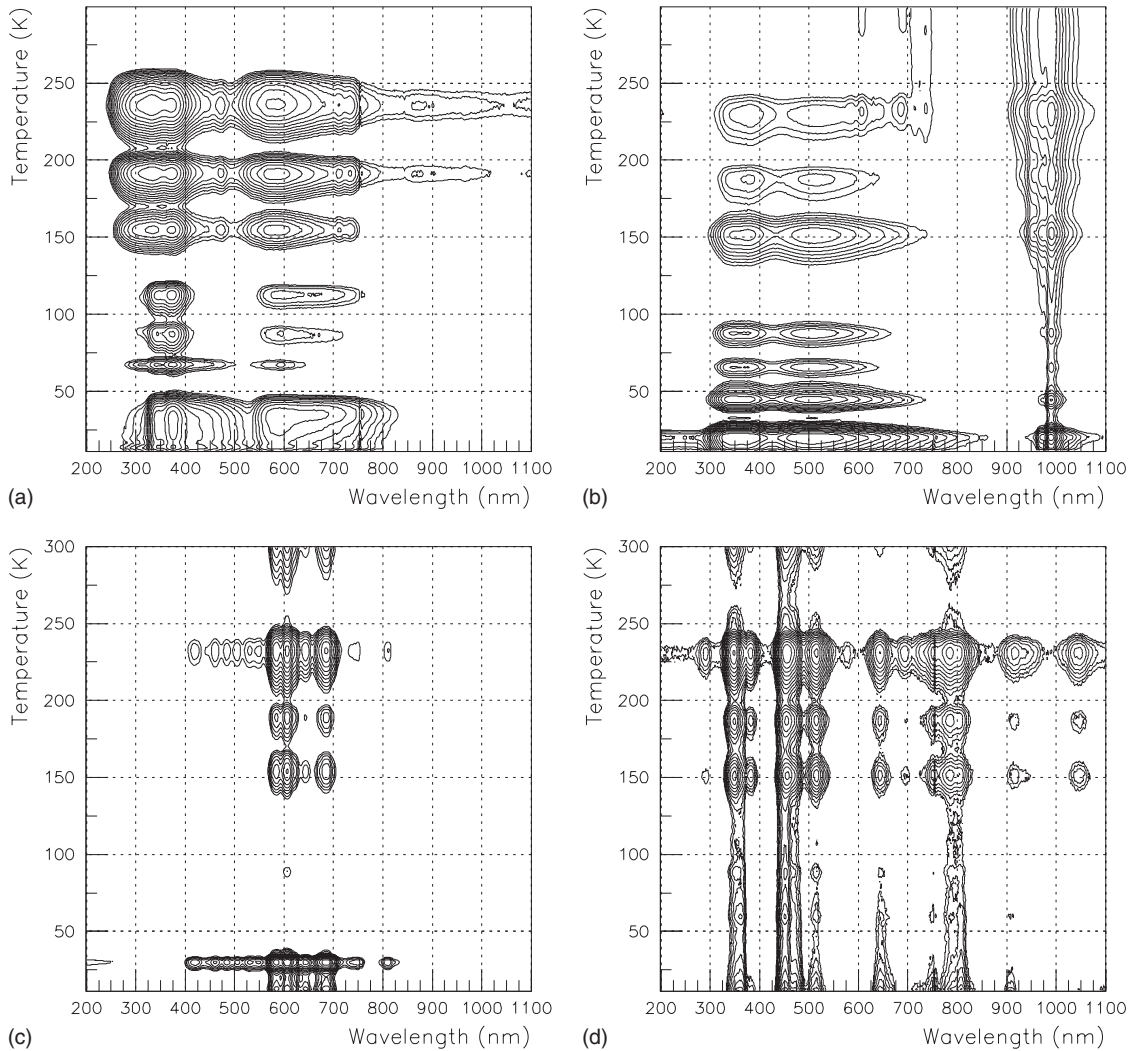


FIG. 1. Contour plots of wavelength-resolved TSL measurements performed after x-ray irradiation at 10 K in (a) undoped YAP; (b) 2% Yb; (c) 0.1% Eu; (d) 0.1% Tm. Heating rate=0.1 K/s.

(ii) the Yb^{3+} charge-transfer (CT) bands at ~ 3.6 and ~ 2.4 eV and the $4f^{13} {}^3F_{5/2} - 4f^{13} {}^2F_{7/2}$ transition at ~ 1.2 eV in the Yb^{3+} -doped sample [by T increasing the intensity of the $4f^{13} {}^2F_{5/2} - 4f^{13} {}^2F_{7/2}$ lines increases with respect to that of the CT bands, as expected due to the thermally activated energy transfer occurring from CT levels to $4f$ levels as already observed in both garnets and perovskites (Ref. 11)]; (iii) the $4f^6 {}^5D_0 - 4f^6 {}^7F_j$ transitions in the Eu^{3+} -doped crystal. In all spectra the signal above 5 eV is an artifact due to the spectral correction. The spectrum of the undoped crystal is more complicated since it features intrinsic excitonic emission bands in the 4–5 eV region, a defect related composite emission in the 2 eV region, and the characteristic $5d-4f$ emission of Ce^{3+} at 3.3 and 3.6 eV mostly evident for $T < 150$ K. Defects responsible for all glow peaks seem to be intrinsic since the same peaks are found in samples of different origin. Moreover, they appear to act as hole traps; after thermal detrapping, holes recombine with electrons stored in electron traps either of intrinsic (possibly oxygen vacancies as recently proposed)²⁸ or of extrinsic nature (Tm^{3+} , Yb^{3+} , and Eu^{3+} dopants). The involvement of oxygen vacancies (F centers) as intrinsic emission centers is

supported by a previous proposal that excitons in YAP are localized close to F centers,³⁰ and by the recent finding of F -type centers by EPR.²⁸ The dominant recombination mechanism is presumably the thermal detrapping of holes into the valence band prior to their radiative recombination with no (or little) spatial correlation between traps and centers. This assumption is supported by the coexistence in the same glow peaks of several emission bands in the undoped sample and by the common position of glow peaks in the Tm^{3+} -, Yb^{3+} -, and Eu^{3+} -doped crystals. However, we note that in such picture involving holelike traps and electronlike recombination centers, Ce^{3+} emission should not be detected since, as it is well known, due to its electronic configuration this ion acts as a hole trap. The role of Ce^{3+} in the recombination process will be discussed in detail in the next section.

To better visualize the shape of the glow curves, wavelength-resolved measurements of all samples were integrated in their respective emission bands to obtain classical glow curves which are reported in Fig. 3. The general similarity of the glow peak positions is clear, apart from the lowest T region up to 40 K. In this temperature interval we observe a strong signal whose shape changes from crystal to

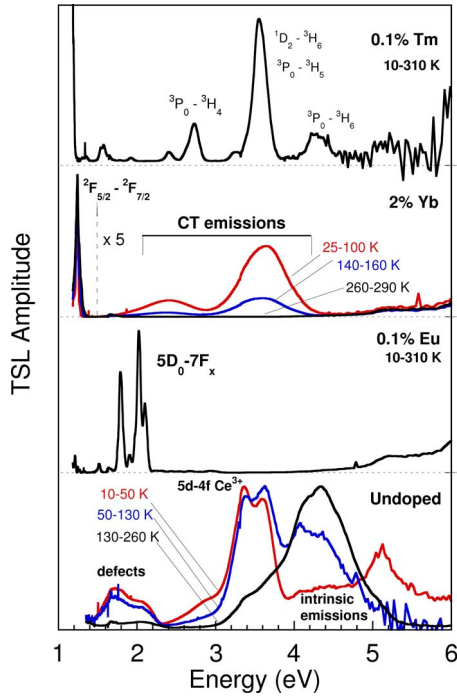


FIG. 2. (Color online) TSL emission spectra of YAP undoped and of Eu-, Yb-, and Tm-doped samples obtained by the integration of wavelength-resolved measurements in the temperature intervals indicated in the graph.

crystal. However, we remark that in this temperature region, being close to the irradiation temperature, the glow curve shape can also be affected by experimental conditions. Considering higher temperatures, peaks are observed at 45, 66, 89, 110, 154, 190, and 232 K in all samples. A shoulder at about 250 K is observed only in the Czochralski grown crystal with the highest (5N) purity (result not shown) while it is absent in all the other samples, both doped and undoped. Moreover, a very broad peak extending from approximately 120 K up to RT is observed in the Yb³⁺-doped crystal. This peak is exclusively related to the 4*f*-4*f* emission of Yb³⁺, as clearly evidenced in Fig. 4. Its broad shape is really uncommon in a crystalline material, where traps, having a well-defined energy depth in the forbidden gap, are expected to give rise to narrower structures as indeed also observed in the same crystal. This result suggests the existence of a further weakly temperature-dependent *e*-*h* recombination path involving selectively the 4*f* excited levels of Yb³⁺.

The trap depths of all peaks were investigated by partial cleaning measurements;³¹ the Arrhenius plots manifesting the exponential rise at the beginning of each peak, from which the trap depths can be evaluated, are displayed in Fig. 5. The figure reports also the calculated energy values ranging from 0.09 (45 K peak) up to 0.62 eV (232 K peak).

Since no shift in the maximum temperatures of the peaks was evidenced by varying the irradiation dose by more than two orders of magnitude, we rely that all traps obey to a first-order recombination process. Therefore the frequency factors *s* of the traps and the RT lifetimes τ can be evaluated by the simple formulas,

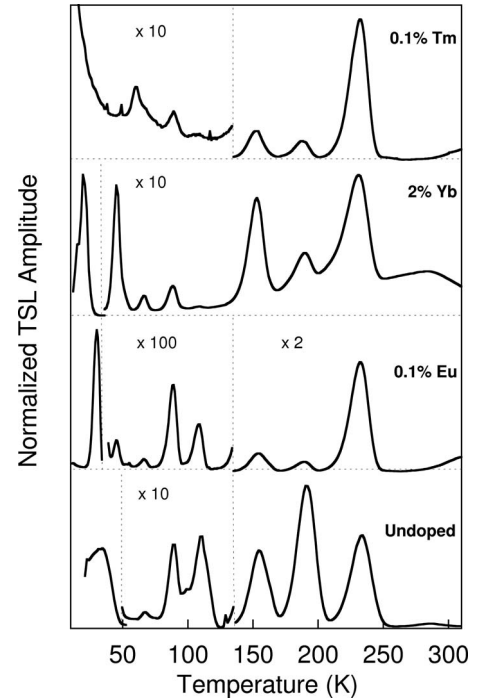


FIG. 3. Glow curves obtained by integration of wavelength-resolved TSL measurements in selected emission regions: 200–800 nm for the undoped sample, 400–900 nm for the 0.1% Eu-doped sample, 270–1050 nm for the 2% Yb-doped sample, and 300–850 nm for the 0.1% Tm-doped sample.

$$s = \frac{\beta E}{kT_m^2} \exp\left(\frac{E}{kT_m}\right), \quad (1)$$

$$\tau = \frac{1}{s} \exp\left(\frac{E}{kT}\right), \quad (2)$$

where β is the heating rate, k is the Boltzmann's constant, and T_m is the temperature at the peak maximum.

The frequency factors and the RT lifetimes of the traps are reported in Table I. We note that no temperature dependence of the frequency factor *s* is considered in the calculation of the RT lifetime due to the lack of specific information, which can hardly be obtained experimentally [Refs. 31 (page 49) and 32]. According to Ref. 31 the temperature dependence should follow a T^a power law with $-2 < a < 2$. So it should not affect the order of magnitude of the calculated frequency factors and of the RT lifetimes of peaks above 100–150 K. In Fig. 6 we show as an example the numerical fit of the glow curve of the Eu³⁺-doped crystal performed in the framework of first-order recombination; the obtained parameters were similar to those reported in Table I. In the fit we did not consider the lowest temperature part of the glow curve up to 40 K due to the influence of experimental conditions in this region, as well as the presence of extremely weak additional structures at the low- and high-*T* side of the 66 K peak.

Our trap depth results for the peaks at 110 and 154 K are in agreement with those reported in Ref. 19 in the case of a 0.3–0.4% Ce³⁺-doped crystal; a difference between the two evaluations is observed only for the frequency factor of the

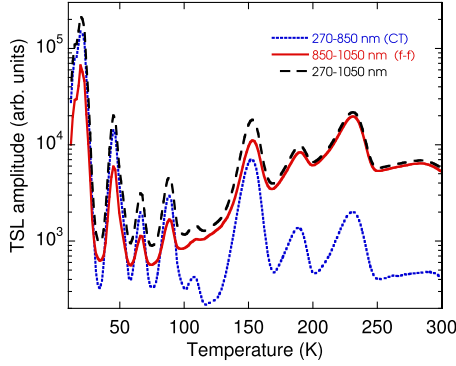


FIG. 4. (Color online) TSL glow curves of 2% Yb-doped YAP integrated in different emission regions reported in the legend.

110 K peak (10^{10} s^{-1} in our calculation with respect to 7×10^{11} in Ref. 19). Consequently the room-temperature lifetimes turn out to be different, 10^3 ns and 82 ns in our evaluation and in Ref. 19, respectively. The very shallow trap with $E=0.13 \text{ eV}$ assumed to exist in Ref. 19 from the temperature dependence of the light yield, yet without any corresponding TSL peak being monitored, could coincide with the traps presently observed with trap depths $E=0.09\text{--}0.15 \text{ eV}$. More significant differences are obtained in comparison with our previous work on a sample doped with 0.5% Ce^{3+} , especially concerning the 110 K peak, which turned out to be characterized by $E=0.18 \text{ eV}$, $s=10^7 \text{ s}^{-1}$.³³ The influence of doping on the TSL peak shape possibly giving rise to such different values will be discussed in the next section.

The traps responsible for TSL peaks at 154, 190, and 232 K are related to three different variants of O^- centers, as shown in Fig. 7 displaying the correspondence between the thermal stabilities of such hole traps detected by EPR and the

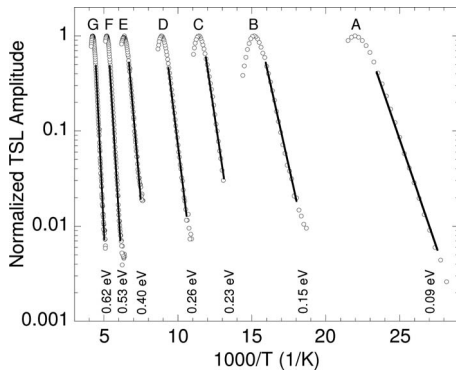


FIG. 5. Arrhenius plots of the TSL of YAP crystals following x-ray irradiation at 10 K and partial cleaning at different T_{stop} temperatures. Curve A, $T_{\text{stop}}=43 \text{ K}$ (45 K peak); curve B, $T_{\text{stop}}=63 \text{ K}$ (66 K peak); curve C, $T_{\text{stop}}=85 \text{ K}$ (89 K peak); curve D, $T_{\text{stop}}=106 \text{ K}$ (110 K peak); curve E, $T_{\text{stop}}=150 \text{ K}$ (154 K peak); curve F, $T_{\text{stop}}=185 \text{ K}$ (190 K peak); curve G, $T_{\text{stop}}=228 \text{ K}$ (232 K peak). The curves are normalized to their maximum. Continuous lines are fits to the data by a single exponential function. The trap-depths values calculated for each peak are also reported. For the 45, 66, and 89 K peaks, data from the 2% Yb-doped sample were considered while for those at 110, 154, 189, and 232 K the analysis was performed for the undoped crystal.

TABLE I. Trap-depths parameters of the TSL peaks observed in YAP crystals after x-ray irradiation at 10 K. The error of the trap depths (E) is approximately 10%. The values of the frequency factors and of the room-temperature lifetimes are more qualitative (only the orders of magnitude are significant). Heating rate of the TSL measurements= 0.1 K/s .

TSL peak temperature (K)	E (eV)	s (1/s)	τ at 293 K (s)
45	0.09	10^7	10^{-7}
66	0.15	10^{10}	10^{-8}
89	0.23	10^{11}	10^{-8}
110	0.26	10^{10}	10^{-6}
154	0.40	10^{11}	10^{-5}
190	0.53	10^{12}	10^{-3}
232	0.62	10^{11}	10^{-1}

TSL glow peaks. It was already proposed for undoped samples that during the TSL process the holes freed from O^- centers recombine with electrons stored in oxygen vacancies.²⁸ The results obtained here for crystals doped with Yb^{3+} , Eu^{3+} , and Tm^{3+} are in agreement with this picture. The observation of the characteristic spectra of these rare earth ions in the TSL emission demonstrates that, after capturing electrons during irradiation (so becoming temporarily $2+$), they compete with intrinsic defects and play the role of recombination centers in the TSL process. The nature of defects responsible for lower temperature peaks at 45, 66, 89, and 110 K is so far not known. Due to the similarity of their emission spectra with those of the other higher temperature peaks, one may suggest that they belong to hole traps as well.

B. Crystals doped with Ce^{3+} , Pr^{3+} , and Tb^{3+}

The glow curves of crystals doped with rare earth ions which are expected to act as hole traps during ionizing irradiation such as Ce^{3+} , Pr^{3+} , and Tb^{3+} were also investigated. In principle, a competition between these activators and precursors of intrinsic hole centers (O^- in our case) is likely to

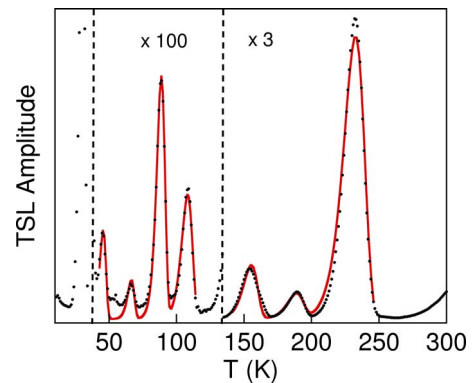


FIG. 6. (Color online) TSL glow curve of YAP: 0.1% Eu (full circles). The continuous (red) line represents the numerical fit of the glow curve in the framework of first-order kinetics.

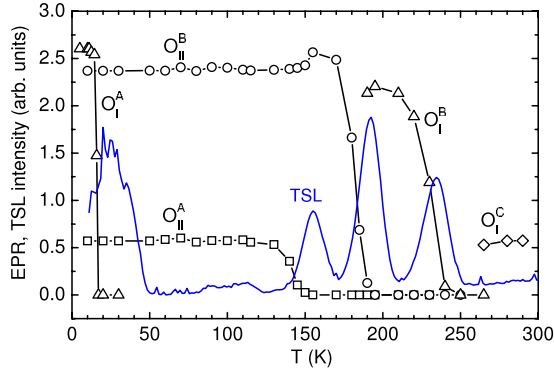


FIG. 7. (Color online) Comparison between the temperature stability of O^- centers obtained from EPR by the isochronal annealing method and TSL glow peaks in undoped YAP. TSL peaks are slightly shifted with respect to mean temperatures of the EPR intensity decay due to differences in the experimental conditions used in both methods (continuous sample heating in TSL and isochronal annealing in EPR).

occur. Such competition should result in a different TSL pattern with respect to that observed for undoped or Yb^{3+} -, Eu^{3+} -, and Tm^{3+} -doped crystals. In particular, glow peaks related to electrons freed from electron traps and undergoing recombination at luminescent ions (temporarily Ce^{4+} , Pr^{4+} , or Tb^{4+}) are expected to occur.

Interestingly, the glow curves of all samples (with 0.1% concentration of the selected rare earth) reported in Fig. 8 in comparison with that of an undoped crystal show an unex-

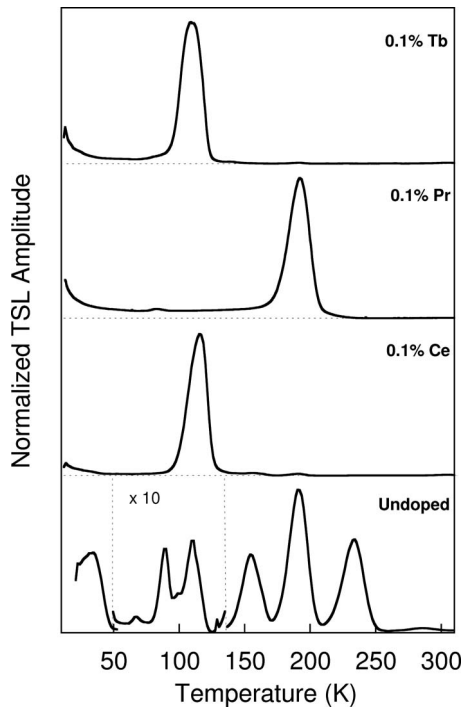


FIG. 8. Glow curves obtained by integration of TSL wavelength-resolved measurements in selected emission regions: 200–800 nm for the undoped sample, 300–450 nm for the 0.1% Ce-doped sample, 350–900 nm for the 0.1% Pr-doped sample, and 350–650 nm for the 0.1% Tb-doped sample.

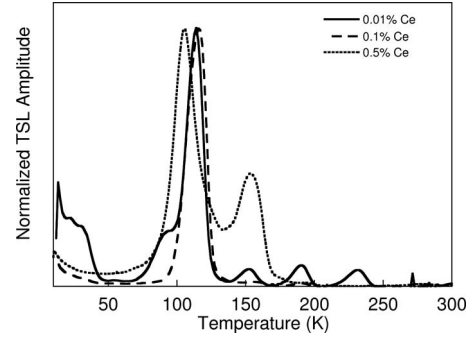
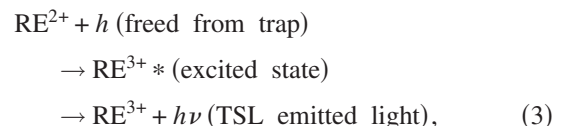


FIG. 9. Comparison between the TSL glow curves of YAP samples with different Ce concentrations obtained after x-ray irradiation at 10 K.

pected shape. Each glow curve features mainly a single peak, preceded by a nearly temperature-independent weak emission starting from 10 K and completely suppressed after the glow peak. The single peaks in different samples coincide with one of those observed in the undoped crystal, namely, with either the 110 K peak for Ce and Tb doping or the 190 K peak for Pr doping. Other peaks, like those at 154 and 190 K in the Ce-doped sample, and at about 82 K in the Pr-doped one, can only barely be noticed. Moreover, in Fig. 9 the glow curves of three samples with different Ce concentration are reported. At the lowest Ce concentration (0.01%), all peaks above 110 K are still observed such as in undoped crystals while they disappear in the 0.1% Ce-doped sample. At still higher concentration (0.5%) the main glow peak is slightly shifted to lower temperatures and the one at 154 K is also detected.

For most of the samples the TSL emission is characteristic of the luminescent activators as shown in Fig. 10. For the lowest Ce^{3+} concentration (0.01%) the intrinsic emission is also detected in peaks above 130 K, testifying the residual intrinsic character of this sample due to its very low Ce^{3+} concentration. In the Pr-doped crystal, the $4f-4f$ transitions dominate in the temperature-independent region below 150 K while the $5d-4f$ transitions are the principal emissions at the temperature region close to the TSL peak.

The nearly temperature-independent emission observed in all these samples before the main glow peak can be ascribed to a kind of tunnel recombination between a trap and rare earth ions acting as recombination centers, similarly, for example, to what observed in garnet scintillators.³⁴ On the other hand, the presence of a single peak occurring at the same temperature of one peak among those observed in the set of samples doped with Eu^{3+} , Tm^{3+} , or Yb^{3+} ions is puzzling. In fact, this brings us to suppose that the defects responsible for the 110 and 190 K peaks can trap both electrons and holes in order to satisfy the following substantially opposite recombination reactions with rare earths (RE),



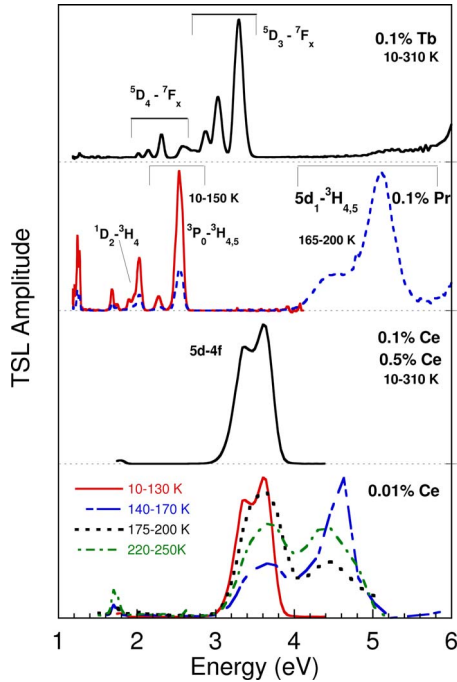
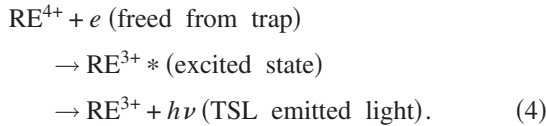


FIG. 10. (Color online) TSL emission spectra of YAP samples doped with Ce, Pr, and Tb obtained by the integration of wavelength-resolved measurements in the temperature intervals indicated in the graph.



In Eq. (3), the RE^{2+} are Eu, Tm, or Yb. In Eq. (4), the RE^{4+} is Ce or Tb for the 110 K peak, and Pr for the 190 K peak.

We will consider several hypotheses to shed light on these results. The casual temperature coincidence of peaks due to electron traps with those due to hole traps detected in $\text{RE}^{3+}/\text{RE}^{2+}$ -doped samples seems unlikely. Not only it requires too much of coincidence (two distinct peaks) but besides, the exclusive presence of the 110 K peak in YAP:Ce(Tb), and of the 190 K peak in YAP:Pr would remain unexplained. The possibility that Ce, Tb, and Pr ions trap electrons during irradiation could, in principle, be taken into account, especially for the last two ions for which a stable $2+$ configuration in wide band-gap insulators was predicted.³⁵ However, if such hypothesis is supposed to work the Ce-, Tb-, and Pr-doped crystals are expected to behave like those doped with Yb, Eu, and Tm, showing accordingly all hole-related glow peaks. As a result, neither the exclusive presence of a single peak nor the existence of the temperature-independent emission get justified.

A more complex interpretation could be based on the following possibility. Suppose the TSL in $\text{RE}^{3+}/\text{RE}^{4+}$ -doped samples involves hole traps and the emitted light is primarily due to intrinsic recombination centers. These intrinsic emissions are then converted in the RE spectra by a reabsorption mechanism leading to RE excitation and subsequent emission from their excited states. To verify this hypothesis we

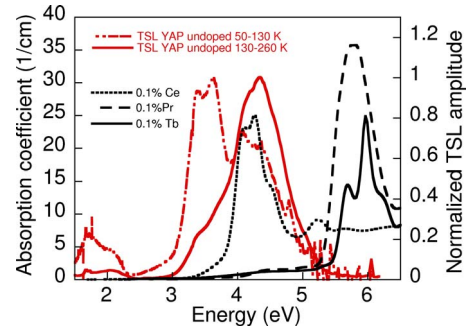


FIG. 11. (Color online) Left ordinate scale, optical-absorption spectra of Ce-, Pr-, and Tb-doped YAP (black curves); right ordinate scale, TSL emissions of undoped YAP in the 50–130 K and 130–260 K intervals (red curves).

compared the absorption spectra of Ce-, Tb-, and Pr-doped samples with the intrinsic TSL emission monitored in the undoped sample (Fig. 11): a reabsorption process is likely to occur only in the case of Ce doping since its $4f$ - $5d$ transitions overlap with intrinsic emissions while $4f$ - $5d$ transitions of Pr and Tb lie at clearly higher energies.

Alternatively, we may propose a reasonable although only qualitative interpretation based on the existence of defect complexes involving intrinsic defects coupled to rare earth ions. Namely, we suggest that Ce, Pr, and Tb dopants are located close to intrinsic hole traps (O^- for the 190 K peak) and electron traps (for example, F centers) so to form a complex in which carriers can be transferred from intrinsic energy levels to the rare earth ion energy levels. Furthermore, in order to explain the existence of only one TSL peak, we assume that the presence of the RE favors the formation of a specific hole-center configuration among those monitored in undoped and in Eu-, Tm-, and Yb-doped crystals. After irradiation at low temperatures, part of holes and electrons are transferred toward the RE ground and excited states, respectively, where they radiatively recombine producing an athermal emission characterized by the RE emission spectrum. As the temperature is gradually raised close to the maximum temperature of the corresponding TSL peak, holes experience also thermal liberation from intrinsic hole centers triggering the liberation of closely lying trapped electrons too, which radiatively recombine at the rare earth site. The rare earth ion works in the defect complex such as an antenna attracting the carriers previously localized in closely spaced lattice defects and promoting their radiative recombination. The appearance of the 154 K peak in YAP 0.5% Ce^{3+} not detected in YAP:0.1% Ce^{3+} (Fig. 9) could be due to the progressive formation of defect complexes involving the $\text{O}_{\text{II}}^{\text{A}}$ defects by increasing Ce concentration. However, recent EPR measurements revealed that this center, as well as other O^- variants, is not visible in Ce-doped crystals. On the other hand, the trapping of a hole by an oxygen ion in the vicinity of Ce^{3+} could occur, leading to the creation of $\text{Ce}^{3+}\text{-O}^-$ centers. Probably such a center is not observable by EPR due to the strong exchange interaction between the spins of O^- and Ce^{3+} ions.

In this framework we can also discuss the shape of the TSL peaks. In Figs. 12(a)–12(c) we report the details of the

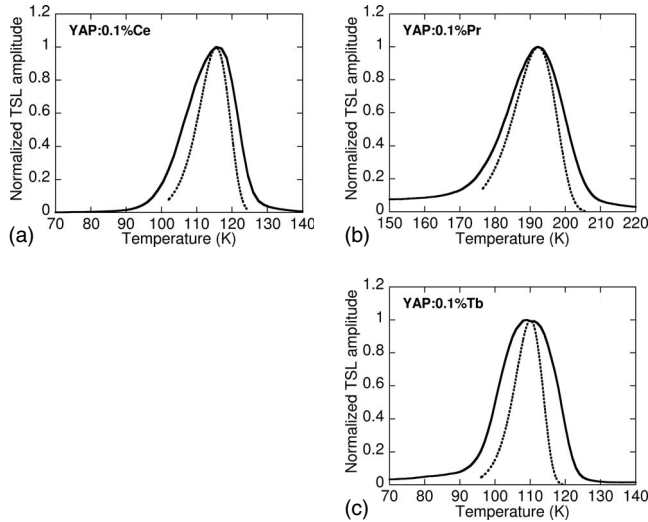


FIG. 12. Detail of the TSL glow curves of (a) YAP 0.1 % Ce, (b) YAP:0.1% Pr, and (c) YAP:0.1% Tb. Continuous line, experimental data; dashed line, numerical simulation with peak parameters from Table I.

TSL peaks for Ce, Pr, and Tb dopings together with a simulation performed with the parameters listed in Table I and obtained for undoped and $\text{RE}^{3+}/\text{RE}^{2+}$ -doped samples. We notice that the peak position of each simulated curve agrees with that of the corresponding experimental curve. Nevertheless, the simulations considerably fail to reproduce the shape of the peaks being in reality evidently broader. A similar result was already obtained in Ref. 19 for a Ce-doped crystal and attributed to the existence of a distribution of trap levels centered around a specific couple of E and s values found in agreement with the temperature dependence of the light yield (namely, $E=0.28$ eV, $s=7 \times 10^{11}$ s $^{-1}$). We confirm the broad shape of the peak for Ce^{3+} doping and we extend the same result also to the cases of Tb^{3+} and Pr^{3+} ; moreover we suggest that its origin lies in the existence of complexes including intrinsic defects and rare earths in which the TSL recombination process does not follow a classical recombination kinetics. This is also testified by the presence of a nearly athermal emission at lower temperatures, which completely disappears above the peak maximum. The independent analysis of these glow peaks both by the aid of the initial rise method and by numerical fit gave much lower energies (lower or equal to 0.2 eV for the 110 K peak and about 0.42 eV for the 190 K peak) and lower frequency factors with respect to those reported in Table I (of the order of 10^3 – 10^6 s $^{-1}$ for the 110 K peak and 10^9 s $^{-1}$ for the 190 K one). However we think that such couples of parameters have poor physical meaning and they just serve to account for anomalously broad peaks associated to traps which do not obey to a classical recombination process.

We note that the existence of defect complexes was already proposed to explain particular TSL phenomena such as the dependence of peaks maximum temperatures upon rare earth ions radii and concentration.^{36–38} As pointed out before, the lack of observation of O^- defects in Ce^{3+} -doped crystals could be explained by the vicinity of O^- centers and Ce ions which may change the EPR-observable characteristics.

IV. CONCLUSIONS

The processes of trapping and recombination of free carriers created by ionizing irradiation in an important scintillator material such as YAlO_3 have been investigated by studying crystals doped with a large variety of rare earth ions. Our TSL results demonstrate that intrinsic defects trapping holes during irradiation are responsible for seven glow peaks from 10 to 300 K; rare earth ions trapping preferably electrons such as Eu, Tm, and Yb act as TSL recombination centers.

On the other hand, Ce-, Pr-, and Tb-doped crystals feature only one principal peak, which coincides with one of those observed in undoped or Eu-, Tm-, Yb-doped crystals. The peak is preceded by a nearly temperature-independent emission which disappears after the glow peak. Such observation is not consistent with a classical TSL picture: in fact, rare earth ions which trap holes during ionizing irradiation such as Ce, Pr, and Tb are expected to compete with intrinsic hole traps in carrier capture giving rise to a different TSL pattern with respect to that of the dopants above. Such TSL pattern would be mostly related to electrons escaping from electron traps and recombining with holes at Ce, Pr, or Tb sites. After considering several possible hypotheses, we suggest that the observed effects could be explained by considering that traps and recombination centers do not act like separate entities, but rather as parts of defect complexes in which carriers can be transferred from intrinsic levels to the rare earth ion levels. The observation of a nearly temperature-independent TSL emission suggests that tunneling-driven recombination processes occur in addition to the temperature-driven recombination, supporting the existence of such complexes with close spatial correlation between traps and centers. The comparison of the TSL patterns of crystals doped with a variety of rare earth ions proved to be essential in order to highlight this phenomenology, which nevertheless could be more common in TSL experiments than expected.

ACKNOWLEDGMENTS

The authors gratefully acknowledge the financial support of the CARIPLO Foundation project “Energy transfer and trapping processes in nanostructured scintillator materials” (2008–2011). The financial support of the Czech Project (Project No. GA AV IAA100100810) and MSMT, KONTAKT under Project No. ME953 is also gratefully acknowledged.

- ¹A. Lempicki, A. Wojtowicz, and E. Berman, *Nucl. Instrum. Methods Phys. Res. A* **333**, 304 (1993).
- ²M. J. Weber, *J. Appl. Phys.* **44**, 3205 (1973).
- ³J. A. Mareš, M. Nikl, C. Pédrini, B. Moine, and K. Blažek, *Mater. Chem. Phys.* **32**, 342 (1992).
- ⁴V. G. Baryshevsky, M. V. Korzhik, B. I. Minkov, S. A. Smirnova, A. A. Fyodorov, P. Dorenbos, and C. W. E. van Eijk, *J. Phys.: Condens. Matter* **5**, 7893 (1993).
- ⁵Y. Zorenko, V. Gorbenko, I. Konstankevych, T. Voznjak, V. Savchyn, M. Nikl, J. A. Mares, K. Nejezchleb, V. Mikhailin, V. Kolobanov, and D. Spassky, *Radiat. Meas.* **42**, 528 (2007).
- ⁶M. Zhuravleva, A. Novoselov, E. Mihokova, J. A. Mares, A. Vedda, M. Nikl, and A. Yoshikawa, *Cryst. Res. Technol.* **42**, 1324 (2007).
- ⁷M. Zhuravleva, A. Novoselov, E. Mihokova, J. A. Mares, A. Vedda, M. Nikl, and A. Yoshikawa, *IEEE Trans. Nucl. Sci.* **55**, 1476 (2008).
- ⁸I. A. Kamenskikh, N. Guerassimova, C. Dujardin, N. Garnier, G. Ledoux, C. Pédrini, M. Kirm, A. Petrosyan, and D. Spassky, *Opt. Mater.* **24**, 267 (2003).
- ⁹M. Nikl, N. Solovieva, J. Pejchal, J. B. Shim, A. Yoshikawa, T. Fukuda, A. Vedda, M. Martini, and D. H. Yoon, *Appl. Phys. Lett.* **84**, 882 (2004).
- ¹⁰J. B. Shim, A. Yoshikawa, M. Nikl, J. Pejchal, A. Vedda, and T. Fukuda, *Radiat. Meas.* **38**, 493 (2004).
- ¹¹I. A. Kamenskikh, C. Dujardin, N. Garnier, N. Guerassimova, G. Ledoux, V. Mikhailin, C. Pédrini, A. Petrosyan, and A. Vasil'ev, *J. Phys.: Condens. Matter* **17**, 5587 (2005).
- ¹²A. G. Petrosyan, G. O. Shirinyan, C. Pedrini, C. Durjardin, K. L. Ovanesyan, R. G. Manucharyan, T. I. Butaeva, and M. V. Derzyan, *Cryst. Res. Technol.* **33**, 241 (1998).
- ¹³J. A. Mareš, N. Čechová, M. Nikl, J. Kvapil, R. Krátký, and J. Pospíšil, *J. Alloys Compd.* **275-277**, 200 (1998).
- ¹⁴A. G. Petrosyan, G. O. Shyrinyan, K. L. Ovanesyan, C. Pedrini, and C. Dujardin, *J. Cryst. Growth* **198-199**, 492 (1999).
- ¹⁵J. Chval, D. Clement, J. Giba, J. Hybler, J.-F. Loude, J. A. Mares, E. Mihokova, C. Morel, K. Nejezchleb, A. Vedda, and H. Zaidi, *Nucl. Instrum. Methods Phys. Res. A*, **443**, 331 (2000).
- ¹⁶J. Trummer, E. Auffray, P. Lecoq, A. G. Petrosyan, and P. Sempere-Roldan, *Nucl. Instrum. Methods Phys. Res. A* **551**, 339 (2005).
- ¹⁷C. Dujardin, C. Pédrini, J. C. Gacon, A. G. Petrosyan, A. N. Belsky, and A. N. Vasil'ev, *J. Phys.: Condens. Matter* **9**, 5229 (1997).
- ¹⁸A. J. Wojtowicz, J. Glodo, W. Drozdowski, and K. R. Przegietka, *J. Lumin.* **79**, 275 (1998).
- ¹⁹A. J. Wojtowicz, J. Glodo, A. Lempicki, and C. Brecher, *J. Phys.: Condens. Matter* **10**, 8401 (1998).
- ²⁰A. J. Wojtowicz, P. Szupryczynski, D. Wisniewski, J. Glodo, and W. Drozdowski, *J. Phys.: Condens. Matter* **13**, 9599 (2001).
- ²¹R. H. Bartram, D. S. Hamilton, L. A. Kappers, and A. Lempicki, *J. Lumin.* **75**, 183 (1997).
- ²²C. R. Stanek, K. J. McClellan, M. R. Levy, and R. W. Grimes, *J. Appl. Phys.* **99**, 113518 (2006).
- ²³M. M. Kuklja, *J. Phys.: Condens. Matter* **12**, 2953 (2000).
- ²⁴D. J. Singh, *Phys. Rev. B* **76**, 214115 (2007).
- ²⁵M. Nikl, J. A. Mares, J. Chval, E. Mihokova, N. Solovieva, M. Martini, A. Vedda, K. Blazek, P. Maly, K. Nejezchleb, P. Fabeni, G. P. Pazzi, V. Babin, K. Kalder, A. Krasnikov, S. Zazubovich, and C. D'Ambrosio, *Nucl. Instrum. Methods Phys. Res. A* **486**, 250 (2002).
- ²⁶C. R. Stanek, M. R. Levy, K. J. McClellan, B. P. Uberuaga, and R. W. Grimes, *Phys. Status Solidi B* **242**, R113 (2005).
- ²⁷O. F. Schirmer, K. W. Blazey, and W. Berlinger, *Phys. Rev. B* **11**, 4201 (1975).
- ²⁸M. Nikl, V. V. Laguta, and A. Vedda, *Phys. Status Solidi B* **245**, 1701 (2008).
- ²⁹A. Vedda, M. Martini, F. Meinardi, J. Chval, M. Dusek, J. A. Mares, E. Mihokova, and M. Nikl, *Phys. Rev. B* **61**, 8081 (2000).
- ³⁰Yu. Zorenko, A. S. Voloshinovskii, I. V. Konstankevych, G. B. Striganyuk, and V. I. Gorbenko, *Opt. Spectrosc.* **98**, 555 (2005).
- ³¹S. W. S. Mc Keever, *Thermoluminescence of Solids* (Cambridge University Press, Cambridge, 1985).
- ³²R. J. Fleming, *J. Phys. D* **23**, 950 (1990).
- ³³M. Fasoli, I. Fontana, F. Moretti, A. Vedda, M. Nikl, E. Mihokova, Y. V. Zorenko, and V. I. Gorbenko, *IEEE Trans. Nucl. Sci.* **55**, 1114 (2008).
- ³⁴M. Nikl, A. Vedda, M. Fasoli, I. Fontana, V. V. Laguta, E. Mihokova, J. Pejchal, J. Rosa, and K. Nejezchleb, *Phys. Rev. B* **76**, 195121 (2007).
- ³⁵P. Dorenbos, *J. Phys.: Condens. Matter* **15**, 8417 (2003).
- ³⁶B. Yang, P. D. Townsend, and A. P. Rowlands, *Phys. Rev. B* **57**, 178 (1998).
- ³⁷P. D. Townsend and A. P. Rowlands, *Radiat. Prot. Dosim.* **84**, 7 (1999).
- ³⁸B. Yang and P. D. Townsend, *J. Appl. Phys.* **88**, 6395 (2000).